Azimuthal asymmetry in lepton-proton scattering at high energies

Junegone Chay, Stephen D. Ellis, and W. James Stirling*
Department of Physics, FM-15, University of Washington, Seattle, Washington 98195
(Received 15 July 1991)

We consider the azimuthal angular dependence of the distribution of final-state hadrons in high-energy lepton-proton scattering. The distribution displays an azimuthal asymmetry due to both perturbative and nonperturbative effects. At the large momentum transfers attainable, for example, at the DESY *ep* collider HERA we expect the perturbative effects to dominate and constitute a clear test of QCD.

PACS number(s): 13.60.Hb, 12.38.Bx, 12.38.Lg

I. INTRODUCTION

The application of the parton model combined with quantum chromodynamics (QCD) has exhibited considerable success in describing high-energy processes such as deep-inelastic leptoproduction. This picture allows us to isolate the basic pointlike constituent scattering process and express the overall cross section as a convolution of three factors: the distribution function describing the partons in the initial state, the fragmentation function describing the distribution of final-state hadrons arising from the scattered parton, and the parton-lepton hard-scattering cross section.

Georgi and Politzer [1] proposed the semi-inclusive leptoproduction process $\ell + p \to \ell' + h + X$, where ℓ, ℓ' are charged leptons and h is a detected hadron, as a clean test of perturbative QCD. In particular, they focused on the azimuthal angular dependence of the hadrons. The z axis is chosen to be in the direction opposite to the three-momentum transfer from the leptons, $\mathbf{q}$, and the x-z plane to be the lepton scattering plane, with the incident and outgoing leptons having positive x components of momenta. In this system the azimuthal angle ϕ of the observed hadron about the z axis can be measured with respect to the x axis.

Cahn [2] expanded the problem by considering the azimuthal angular dependence due to the intrinsic transverse momentum of the partons bound inside the proton. Because of this intrinsic momentum, perturbative QCD alone does not describe the observed azimuthal angular dependence. Berger [3] considered the influence of final-state interactions in the specific instance of the leptoproduction of a pion. The azimuthal asymmetry due to this final-state interaction is opposite in sign to that due to the effects studied by Cahn. The azimuthal asymmetries discussed by both Cahn and Berger are due to nonperturbative effects. In the kinematic regime attainable at the DESY *ep* collider HERA we expect that the perturbative QCD effects will dominate the nonperturbative effects, which are described by higher-twist operators in the operator-product expansion. This is the motivation for considering the azimuthal dependence of final hadrons in *ep* scattering at HERA. We consider in some detail the transition from the lower-momentum regime, where nonperturbative effects dominate, to the purely perturbative regime.

In Sec. II, we review the kinematics of leptoproduction. In Sec. III, we define $\langle \cos\phi \rangle$ and discuss nonperturbative and perturbative contributions to it. An intuitive explanation of the azimuthal asymmetry is provided in Sec. IV. In Sec. V, we present a numerical analysis of $\langle \cos\phi \rangle$ and compare our results with the data obtained recently by the E665 Collaboration [4] at Fermilab. We also discuss the behavior of $\langle \cos\phi \rangle$ at large momentum transfer. In the last section, we conclude that perturbative QCD effects dominate in the kinematic regime that will be accessible at HERA.

II. CROSS SECTIONS

Let k_1 (k_2) be the initial (final) momentum of the lepton, P_1 (P_2) be the target (observed final-state hadron) momentum and p_1 (p_2) be the incident (scattered) parton momentum. At high energy, the hadrons will be produced with momenta nearly parallel to the virtual-photon direction, $q^\mu = k_1^\mu - k_2^\mu$. We are interested in interactions that generate nonzero transverse momentum $\mathbf{P}_{2T}$, perpendicular to $\mathbf{q}$. We can write the differential scattering cross section in terms of the laboratory variables

$$Q^2 = -q^2, \quad \mathbf{P}_T = \mathbf{P}_{2T}, \quad \phi, \tag{1}$$

$$x_H = \frac{Q^2}{2P_1 \cdot q}, \quad y = \frac{P_1 \cdot q}{P_1 \cdot k_1}, \quad z_H = \frac{P_1 \cdot P_2}{P_1 \cdot q},$$

and the parton variables

$$x = \frac{x_H}{\xi} = \frac{Q^2}{2p_1 \cdot q}, \quad z = \frac{z_H}{\xi'} = \frac{p_1 \cdot p_2}{p_1 \cdot q}. \tag{2}$$

The azimuthal angle ϕ of the outgoing hadron is measured with respect to $\mathbf{k}_{1T}$.

In the parton model, the semi-inclusive scattering cross section can be written in terms of the parton variables:

*Permanent address: Depts. of Physics and Mathematical Sciences, University of Durham, Durham, England.

$$\frac{d\sigma}{dx_H\,dy\,dz_H\,d^2P_T} = \sum_{i,j} dx\,dz\,d^2p_T\,d\xi\,d\xi'\,\delta(x_H-\xi x)\delta(z_H-\xi' z)\delta^2(\mathbf{P}_T-\xi'\mathbf{p}_T)F_i(\xi,Q^2)\frac{d\hat{\sigma}_{ij}}{dx\,dy\,dz\,d^2p_T}D_j(\xi',Q^2)\,, \tag{3}$$

with $d^2P_T = P_T dP_T d\phi$. The sum over i and j runs over all types of partons (quarks, antiquarks, and gluons). The cross section $d\hat{\sigma}_{ij}$ describes the partonic semi-inclusive process

$$\ell(k_1)+i(p_1)\to\ell(k_2)+j(p_2)+X\,. \tag{4}$$

$F_i(\xi,Q^2)$ is the probability distribution describing an i-type parton with a fraction ξ of the target's momentum, $p_1^\mu=\xi P_1^\mu$, and $D_j(\xi',Q^2)$ is the probability distribution for a j-type parton to fragment producing a hadron with a fraction ξ' of the parton's momentum, $P_2^\mu=\xi' p_2^\mu$. Both $d\hat{\sigma}_{ij}$ and the Q^2 dependence of F_i and D_j can be calculated in QCD perturbation theory. It has been shown [5] that, to lowest nontrivial order in α_s, the factorization exhibited in Eq. (3) obtains and all large logarithms can be absorbed in F_i and D_j. In Eq. (3) higher-twist effects are neglected.

In zeroth order in α_s, the parton cross section is given by

$$\frac{d\hat{\sigma}_{ij}}{dx\,dy\,dz\,d^2p_T} = \frac{2\pi\alpha^2}{yQ^2}[1+(1-y)^2] \times Q_i^2\delta_{ij}\delta(1-x)\delta(1-z)\delta^2(\mathbf{p}_T), \tag{5}$$

where the Q_i are the electric charges of the quarks (in units of e). Inserting Eq. (5) into Eq. (3), we get the standard result

$$\frac{d\sigma}{dx_H\,dy\,dz_H\,d^2P_T} = \frac{2\pi\alpha^2}{yQ^2}[1+(1-y)^2]\delta^2(\mathbf{P}_T) \times\sum_i Q_i^2F_i(x_H,Q^2)D_i(z_H,Q^2). \tag{6}$$

Note that the transverse momentum $\mathbf{P}_T$ vanishes in the zeroth order in α_s.

To first order in α_s the parton scattering processes develop nonzero p_T and nontrivial ϕ dependence. The relevant processes are

$$q(p_1)+\gamma^*(q)\to q(p_2)+g(p_3), \tag{7}$$
$$q(p_1)+\gamma^*(q)\to q(p_3)+g(p_2), \tag{8}$$
$$g(p_1)+\gamma^*(q)\to q+\bar{q}, \tag{9}$$

where q is a quark or an antiquark, g is a gluon and γ^* is the virtual photon.[1] The Feynman diagrams for these processes are shown in Figs. 1(a)–1(c). In terms of the variables defined in Eqs. (1) and (2), we can express p_2 as

$$p_2^\mu=(1-x-z+2xz)p_1^\mu+zq^\mu+\tilde{p}_T^\mu, \tag{10}$$

where $\tilde{p}_T=(0,\mathbf{p}_T,0)$ with $p_1\cdot\tilde{p}_T=q\cdot\tilde{p}_T=0$. For massless partons we have

$$p_T^2=|\mathbf{p}_{2T}|^2=\frac{z(1-x)(1-z)}{x}Q^2\,. \tag{11}$$

Similarly we write

$$k_1^\mu=\frac{x}{y}(2-y)p_1^\mu+\frac{1}{y}q^\mu+\tilde{k}_T^\mu, \tag{12}$$

with $k_T^2=(1-y)Q^2/y^2$, where $\tilde{k}_T$ is defined in the same way as $\tilde{p}_T$. Therefore we find

$$k_1\cdot p_2=\frac{Q^2}{2xy}(1-x-z+2xz-xyz)-\mathbf{k}_T\cdot\mathbf{p}_T, \tag{13}$$

and

$$k_2\cdot p_2=\frac{Q^2}{2xy}[(1-x)(1-y)(1-z)+xz]-\mathbf{k}_T\cdot\mathbf{p}_T\,. \tag{14}$$

The semi-inclusive parton scattering cross section is given by

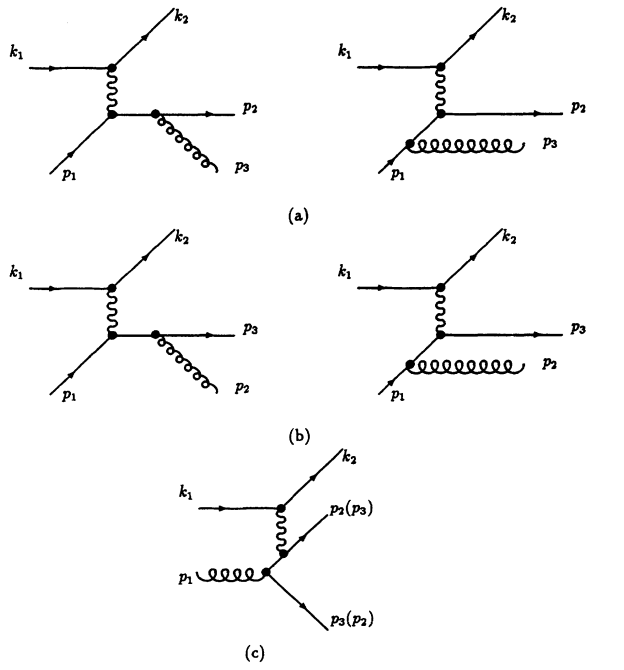

FIG. 1. Feynman diagrams for ℓp scattering at order α_s.

[1] We consider only the electromagnetic case. To be complete, the weak interaction should be included. The weak interaction case is more complicated, but the qualitative features are unchanged.

$$\frac{d\hat{\sigma}_{ij}}{dx\,dy\,dz\,d^2p_T} = \frac{\alpha^2 Q_q^2}{16\pi^2 Q^4} y L_{\mu\nu} M_{ij}^{\mu\nu} \times \delta\left(p_T^2 - \frac{z}{x}(1-x)(1-z)Q^2\right), \quad (15)$$

where $L_{\mu\nu}$ ($M_{ij}^{\mu\nu}$) is the square of the leptonic (partonic) current, α is the electromagnetic fine-structure constant and Q_q is the charge of the scattered quark. $L_{\mu\nu}M_{ij}^{\mu\nu}$ for the processes in Eqs. (7), (8), and (9), i.e., $ij = qq$, qg, and gq, are written as

$$L_{\mu\nu}M_{qq}^{\mu\nu} = \frac{64\pi}{3}\alpha_s Q^2 \frac{(k_1\cdot p_1)^2 + (k_2\cdot p_2)^2 + (k_2\cdot p_1)^2 + (k_1\cdot p_2)^2}{p_1\cdot p_3\; p_2\cdot p_3}, \quad (16)$$

$$L_{\mu\nu}M_{qg}^{\mu\nu} = \frac{64\pi}{3}\alpha_s Q^2 \frac{(k_1\cdot p_1)^2 + (k_2\cdot p_3)^2 + (k_2\cdot p_1)^2 + (k_1\cdot p_3)^2}{p_1\cdot p_2\; p_2\cdot p_3}, \quad (17)$$

$$L_{\mu\nu}M_{gq}^{\mu\nu} = 8\pi\alpha_s Q^2 \frac{(k_1\cdot p_3)^2 + (k_2\cdot p_2)^2 + (k_2\cdot p_3)^2 + (k_1\cdot p_2)^2}{p_1\cdot p_2\; p_1\cdot p_3}. \quad (18)$$

The expression in Eq. (17) is obtained from Eq. (16) by interchanging p_2 and p_3. Figures 2(a)–2(b) exhibit Eq. (16) and Eq. (18) as functions of ϕ for some fixed values of x, y, and z. Note that for an incident q the scattered q tends to appear at ϕ near 180° for all z values. For an incident g the ϕ dependence has the symmetry that $z \leftrightarrow (1-z)$ corresponds to $\phi \leftrightarrow 180° - \phi$.

III. THE DEFINITION OF $\langle\cos\phi\rangle$ AND INTRINSIC TRANSVERSE MOMENTUM

The average value of $\cos\phi$, which measures the front-back asymmetry of $\mathbf{P}_{2T}$ along the $\mathbf{k}_{1T}$ direction, is given by

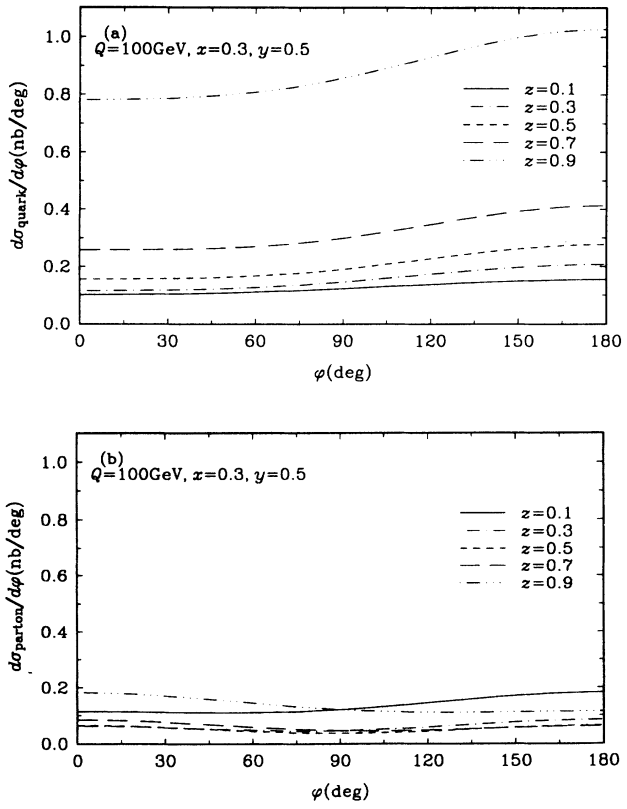

FIG. 2. Parton cross sections as functions of ϕ for (a) $\ell + q \to \ell + q + g$ and (b) $\ell + g \to \ell + q + \bar{q}$.

$$\langle\cos\phi\rangle = \frac{\int d\sigma^{(0)}\cos\phi + \int d\sigma^{(1)}\cos\phi}{\int d\sigma^{(0)} + \int d\sigma^{(1)}}, \quad (19)$$

where $d\sigma^{(0)}(d\sigma^{(1)})$ is the lowest-order (first-order in α_s) hadronic scattering cross section defined in Eq. (3), and the integrations are over P_T, ϕ, x_H, y, and z_H. It follows from Eqs. (5) and (15) that the numerator in Eq. (19) will receive contributions only from the second term (the first term integrates to 0), while the denominator receives contributions from both terms. Thus $\langle\cos\phi\rangle$ is thought of as an order-α_s quantity in perturbation theory. However, this situation can vary significantly when we consider how $\langle\cos\phi\rangle$ is evaluated in actual experiments. The definition of the data set for a typical experiment will generally involve a transverse momentum cutoff p_c. Only hadrons with transverse momenta above the cutoff ($P_T > p_c$) will be included. Since $P_T = 0$ in the zeroth order in α_s, evaluating $\langle\cos\phi\rangle$ for a data sample with $p_c > 0$ implies that there is no contribution from the lowest-order processes to either the numerator or the denominator. Therefore $\langle\cos\phi\rangle$ is independent of α_s at this order in perturbation theory.

However, partons have nonzero transverse momenta as a consequence of being confined by the strong interactions inside hadrons of finite size. The characteristic magnitude of this intrinsic transverse momentum is a few hundred MeV. As Cahn [2] showed, there is a contribution to $\langle\cos\phi\rangle$ from the lowest-order processes due to this intrinsic transverse momentum. Such contributions are generally referred to as higher-twist effects and can, at least formally, be analyzed in the context of the operator-product expansion. We choose to take a more pedestrian but more explicit approach. In order to study the contribution of intrinsic transverse momentum and to explicitly analyze the transition from the nonperturbative to perturbative regimes, we define a simple model of the intrinsic transverse-momentum distribution in both the parton distribution and fragmentation functions. In particular, we assume that the parton distribution, as a function of the intrinsic parton transverse momentum $\boldsymbol{\rho}$, is a product

$$F_i(\xi, Q^2) \to d^2\rho \tilde{F}_i(\xi, \boldsymbol{\rho}, Q^2) = d^2\rho F_i(\xi, Q^2) f(\boldsymbol{\rho}), \quad (20)$$

where the F_i are the previously defined distribution functions. We further assume that $f(\boldsymbol{\rho})$ can be parametrized as a Gaussian,

$$f(\rho) = f(|\rho| = \rho) = \frac{1}{a^2\pi} e^{-\rho^2/a^2}, \tag{21}$$

normalized to unit integral,

$$\int d^2\rho f(\rho) = 1. \tag{22}$$

The average intrinsic transverse momentum is given by $\langle p_T \rangle = a\sqrt{\pi}/2$. [If we use the actual transverse momentum variable $\mathbf{p}_T = \xi\boldsymbol{\rho}$ instead of $\boldsymbol{\rho}$ in Eq. (21), the moments of the distribution functions F_i do not factorize. Therefore we choose the form in Eq. (21) to guarantee the factorization.] We use a similar form for the intrinsic transverse momentum distribution in the fragmentation functions. Again we assume a dependence on only $|\boldsymbol{\rho}'| = \rho'$:

$$D_i(\xi', Q^2) \to d^2\rho'\, \tilde{D}_i(\xi', \rho', Q^2) = d^2\rho'\, D_i(\xi', Q^2) d(\rho'), \tag{23}$$

and

$$d(\rho') = \frac{1}{b^2\pi} e^{-\rho'^2/b^2}, \tag{24}$$

again with unit integral. Note that the two-dimensional transverse momentum $\boldsymbol{\rho}$ ($\boldsymbol{\rho}'$) is defined to be perpendicular to the direction of motion of the incoming proton (outgoing parton). These Gaussian forms are, in fact, motivated by experimental measurements of intrinsic transverse momentum effects in, e.g., Drell-Yan and jet fragmentation experiments. They also have the virtues of being simple and of providing an easily understood and *qualitatively accurate* description of the experimentally observed behavior of $\langle \cos\phi \rangle$ at low values of Q and of the transverse momentum cutoff, where nonperturbative effects dominate. At large values of Q, the contribution to $\langle \cos\phi \rangle$ from these intrinsic transverse momenta is, in any case, negligible compared to the order α_s, perturbative result. This will be discussed in detail in Sec. V.

If we allow the initial partons to have intrinsic transverse momentum, $\mathbf{p}_1 = \xi\mathbf{P}_1 + \boldsymbol{\rho}$ with $\mathbf{P}_1 \cdot \boldsymbol{\rho} = 0$, the parton cross section at lowest order is modified to

$$\frac{d\hat{\sigma}_{ij}}{dx\, dy\, dz\, d^2p_T} = \frac{2\pi\alpha^2}{yQ^2} Q_i^2 \delta_{ij} \delta(1-x)\delta(1-z)\delta^2(\mathbf{p}_T - \boldsymbol{\rho}) \times \left(1 + (1-y)^2 - \frac{4\mathbf{p}_T \cdot \hat{\mathbf{x}}}{Q}\sqrt{1-y}(2-y) + \frac{8(\mathbf{p}_T \cdot \hat{\mathbf{x}})^2}{Q^2}(1-y)\right), \tag{25}$$

where $\hat{\mathbf{x}}$ is the unit vector in the direction of the $\mathbf{k}_{1T}$ perpendicular to $\mathbf{q}$. We also have to modify $\delta^2(\mathbf{P}_T - \xi'\mathbf{p}_T)$ in Eq. (3). In the center-of-mass frame of the virtual photon and the incoming proton we can write

$$q_\mu = (q_0, 0, 0, -P_1), \; P_{1\mu} = (E_1, 0, 0, P_1), \tag{26}$$

where, in the limit $M^2/Q^2 \ll 1$, $P_1^2 = Q^2/4x_H(1-x_H)$. Thus the spatial momentum of the struck quark is $\mathbf{p}_2 = \boldsymbol{\rho} - (1-\xi)\mathbf{P}_1$. With the struck quark fragmenting into a hadron according to Eq. (23), the three-momentum of the hadron can be written as

$$\mathbf{P}_2 = \xi'\mathbf{p}_2 + \boldsymbol{\rho}' = \xi'[\boldsymbol{\rho} - (1-\xi)\mathbf{P}_1] + \boldsymbol{\rho}'. \tag{27}$$

Since $\boldsymbol{\rho}'$ is defined to be perpendicular to $\mathbf{p}_2$, we have

$$\boldsymbol{\rho} \cdot \boldsymbol{\rho}' = (1-\xi)\mathbf{P}_1 \cdot \boldsymbol{\rho}'. \tag{28}$$

Thus we can decompose $\boldsymbol{\rho}'$ as

$$\boldsymbol{\rho}' = \left(\boldsymbol{\rho}' - \frac{\mathbf{P}_1 \cdot \boldsymbol{\rho}'}{P_1^2}\mathbf{P}_1\right) + \frac{\mathbf{P}_1 \cdot \boldsymbol{\rho}'}{P_1^2}\mathbf{P}_1, \tag{29}$$

where the vector in the parentheses is perpendicular to $\mathbf{q}$, and the second vector is parallel to $\mathbf{q}$ (and $\mathbf{P}_1$). Therefore the hadron's transverse momentum, perpendicular to $\mathbf{q}$, is given by

$$\mathbf{P}_T = \xi'\boldsymbol{\rho} + \boldsymbol{\rho}' - \frac{\mathbf{P}_1 \cdot \boldsymbol{\rho}'}{P_1^2}\mathbf{P}_1. \tag{30}$$

Using Eq. (28), we can write the magnitude of this vector as

$$P_T^2 = (\xi'\boldsymbol{\rho} + \boldsymbol{\rho}')^2 - \frac{(\mathbf{P}_1 \cdot \boldsymbol{\rho}')^2}{P_1^2} = (\xi'\boldsymbol{\rho} + \boldsymbol{\rho}')^2 - \frac{4x_H}{1-x_H}\frac{(\boldsymbol{\rho} \cdot \boldsymbol{\rho}')^2}{Q^2}. \tag{31}$$

To keep our formulas simple we will neglect the term of the order ρ^2/Q^2 so that $\mathbf{P}_T = \xi'\boldsymbol{\rho} + \boldsymbol{\rho}'$. For average values of ρ and ρ' of the order of 500 MeV with Q larger than a few GeV and with small x_H, the error of this approximation is less than 10%. In the numerical work displayed in the figures we use the full expression of Eq. (31). Using a delta function of the form $\delta^2(\mathbf{P}_T - \xi'\boldsymbol{\rho} - \boldsymbol{\rho}')$ along with the distribution functions of Eq. (20) and the fragmentation functions of Eq. (23), we obtain, including the integrals over ρ and ρ',

$$\int d\sigma^{(0)} \cos\phi = -8\pi\frac{\alpha^2}{Q^2}\frac{(2-y)\sqrt{1-y}}{y}\sum_j Q_j^2 F_j(x_H) D_j(z_H) \frac{a^2 z_H}{Q\sqrt{b^2 + a^2 z_H^2}} \int_{p_c/\sqrt{b^2+a^2z_H^2}}^{\infty} dx\, x^2 e^{-x^2}, \tag{32}$$

where p_c is the transverse momentum cutoff for the observed hadrons. We also have

$$\int d\sigma^{(0)} = 2\pi\frac{\alpha^2}{Q^2}\sum_j Q_j^2 F_j(x_H) D_j(z_H) \exp\left(-\frac{p_c^2}{b^2 + z_H^2 a^2}\right) \times \left\{\frac{1+(1-y)^2}{y} + 4\frac{1-y}{yQ^2}\left[\frac{a^2b^2}{b^2 + z_H^2a^2} + \left(\frac{z_H a^2}{b^2 + z_H^2 a^2}\right)^2 (p_c^2 + b^2 + z_H^2 a^2)\right]\right\}. \tag{33}$$

Thus we see that including intrinsic transverse momentum leads to a nonzero, negative $\langle\cos\phi\rangle$ even for the lowest-order cross section, as was already clear from Eq. (25).

With the typical sizes of a and b of the order of a few hundred MeV, we expect that for $p_c \gtrsim 2$ GeV the contributions from $\sigma^{(0)}$ [Eq. (32), Eq. (33)] are negligible compared to those from $\sigma^{(1)}$. The intrinsic transverse momenta of the partons simply cannot produce hadrons with transverse momenta larger than p_c and the effects from $\sigma^{(0)}$ are exponentially suppressed. Therefore, for p_c larger than 2 GeV, $\langle\cos\phi\rangle$ is, to a good approximation,

$$\langle\cos\phi\rangle \approx \frac{\int d\sigma^{(1)}\cos\phi}{\int d\sigma^{(1)}}. \tag{34}$$

The numerator can be written as

$$\int d\sigma^{(1)}\cos\phi = \int d^2P_T\cos\phi\frac{d\sigma}{dx_H\,dy\,dz_H\,d^2P_T} = \frac{8}{3}\frac{\alpha_s\alpha^2}{Q^2}\frac{(2-y)\sqrt{1-y}}{y}\int_{x_H}^1\frac{dx}{x}\int_{z_H}^1\frac{dz}{z}\sum_j Q_j^2(A_j+B_j+C_j), \tag{35}$$

where

$$A_j = -\sqrt{\frac{xz}{(1-x)(1-z)}}\,[xz+(1-x)(1-z)]\,F_j\left(\frac{x_H}{x},Q^2\right)D_j\left(\frac{z_H}{z},Q^2\right),$$

$$B_j = \sqrt{\frac{x(1-z)}{(1-x)z}}\,[x(1-z)+(1-x)z]\,F_j\left(\frac{x_H}{x},Q^2\right)D_G\left(\frac{z_H}{z},Q^2\right), \tag{36}$$

$$C_j = -\frac{3}{8}\sqrt{\frac{x(1-x)}{z(1-z)}}(1-2x)(1-2z)F_G\left(\frac{x_H}{x},Q^2\right)D_j\left(\frac{z_H}{z},Q^2\right).$$

These expressions are identical with previous perturbative results as in Ref. [1] (except for the sign of C_j) and Ref. [7]. The denominator can likewise be written as

$$\int d\sigma^{(1)} = \int d^2P_T\frac{d\sigma}{dx_H\,dy\,dz_H\,d^2P_T} = \frac{4}{3}\frac{\alpha_s\alpha^2}{Q^2}\frac{1}{y}\int_{x_H}^1\frac{dx}{x}\int_{z_H}^1\frac{dz}{z}\sum_j Q_j^2(A'_j+B'_j+C'_j), \tag{37}$$

where

$$A'_j = F_j\left(\frac{x_H}{x},Q^2\right)\left([1+(1-y)^2]\,\frac{x^2+z^2}{(1-x)(1-z)}+2y^2(1-xz)+4(1-y)(1+3xz)\right)D_j\left(\frac{z_H}{z},Q^2\right),$$

$$B'_j = F_j\left(\frac{x_H}{x},Q^2\right)\left([1+(1-y)^2]\,\frac{x^2+(1-z)^2}{z(1-x)}+2y^2(1-x+xz)+4(1-y)\,[1+3x(1-z)]\right)D_G\left(\frac{z_H}{z},Q^2\right), \tag{38}$$

$$C'_j = \frac{3}{8}F_G\left(\frac{x_H}{x},Q^2\right)\left([1+(1-y)^2]\,[x^2+(1-x)^2]\,\frac{z^2+(1-z)^2}{z(1-z)}+16(1-y)x(1-x)\right)D_j\left(\frac{z_H}{z},Q^2\right).$$

The quantities A, B, and C and those with primes arise from the diagrams Figs. 1(a)–1(c), respectively.

At large z_H, the gluon fragmentation function is expected to be small compared to the quark fragmentation function. Therefore $A_i \gg B_i$ at large z_H, and the struck quarks tend to produce hadrons with negative $\langle\cos\phi\rangle$. The contribution to $\langle\cos\phi\rangle$ from gluons in the target (C_i) can have either sign depending on whether $z > 0.5$ or $z < 0.5$. When we probe the small x_H region where the gluon contribution dominates and integrate over a wide region of z_H, the asymmetry tends to be washed out. It is difficult to obtain precise information on the gluon distribution function at low x_H from the measurement of the asymmetry in the distribution of hadrons. If we choose, e.g., $x_H \geq 0.01$, where the quark distribution functions are larger than the gluon distribution function, perturbative QCD predicts a negative $\langle\cos\phi\rangle$, since the main contribution comes from A_i.

IV. WHY AN ASYMMETRY?

We can understand why there is an asymmetry at order α_s in the context of color coherence at the parton level. It is known that when a quark-antiquark pair is produced in a color-singlet state soft gluons tend to be emitted inside the cone defined by the quark-antiquark pair. The color field interferes constructively inside the cone and destructively outside the cone. In our case, we have an incoming and an outgoing quark [3 in color SU(3)]. However, we can regard the incoming quark as

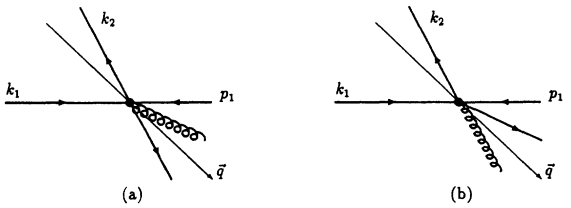

FIG. 3. Two possible cases for the quark and an emitted gluon.

an outgoing antiquark [$\overline{3}$ in color SU(3)] and the pair as a color singlet. Figure 3 shows the configuration of the outgoing quark and an emitted gluon in the center-of-mass frame of the incoming lepton and the incoming proton. Because of the color coherence, the configuration of Fig. 3(a) is more probable than that of Fig. 3(b) because the gluon is inside the cone defined by the quarks. It is exactly this configuration that gives negative $\langle \cos\phi \rangle$ after boosting to the photon-proton cm frame, assuming that we are in a kinematic regime where the observed hadron is coming from the fragmentation of the quark.

For comparison we can consider a "toy" model with scalar gluons. If we assume that the gluon is a scalar particle, A^s, B^s, and C^s corresponding to A, B, and C in Eq. (36) are given by

$$A_i^s = \frac{1}{2}\sqrt{\frac{xz}{(1-x)(1-z)}}\{x+z-2xz\} \times F_i\left(\frac{x_H}{x},Q^2\right) D_i\left(\frac{z_H}{z},Q^2\right),$$

$$B_i^s = -\frac{1}{2}\{(1-x)(1-z)+xz\}\sqrt{\frac{x(1-z)}{(1-x)z}} \times F_i\left(\frac{x_H}{x},Q^2\right) D_G\left(\frac{z_H}{z},Q^2\right), \quad (39)$$

$$C_i^s = 0.$$

If we also assume the scalar gluon to have the same coupling constant, group theory factors, F_G and D_G as the vector gluon, $\langle \cos\phi \rangle$ is positive. Therefore the sign of $\langle \cos\phi \rangle$ itself confirms that the gluon is a vector rather than a scalar particle. The analogous explicit results to Fig. 2 but for this toy scalar model are exhibited in Fig. 4.

V. NUMERICAL ANALYSIS

Finally let us consider how $\langle \cos\phi \rangle$, as defined in Eq. (19) with P_T cutoff p_c, behaves numerically in our simple model including both next-to-leading-order QCD and intrinsic transverse momentum. We use the Harriman-Martin-Roberts-Stirling (HMRS) (set B) parton distribution functions [6] for $F_j(\xi, Q^2)$ in Eq. (20). In order to keep the analysis as simple and transparent as possible, we use analytic parton fragmentation functions. This is to be contrasted with earlier studies using Monte Carlo simulation for the hadronization process [7]. We choose Sehgal's parametrization [8] for the quark fragmentation functions to pions,

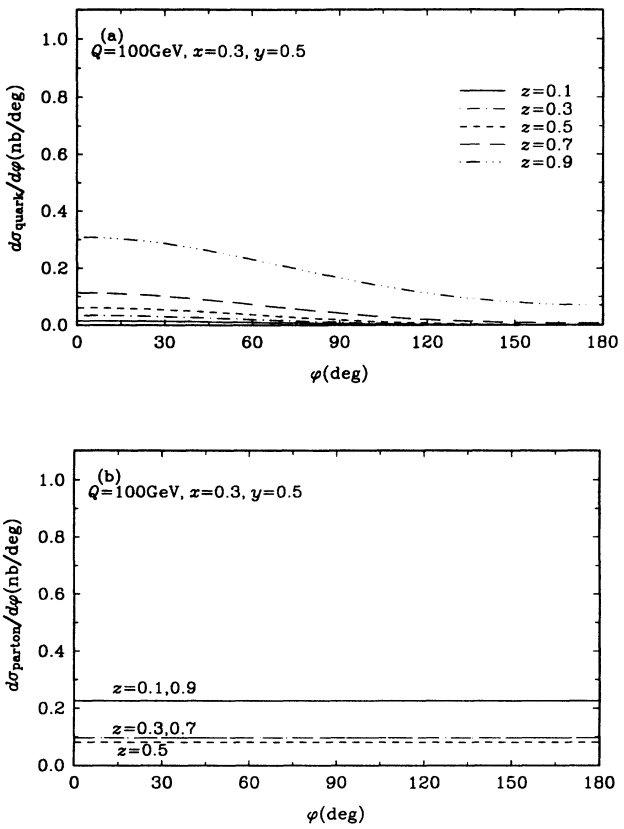

FIG. 4. Parton cross sections for a scalar gluon as functions of ϕ for (a) $\ell + q \to \ell + q + g_s$ and (b) $\ell + g_s \to \ell + q + \bar{q}$.

$$D_j(z) = \frac{1}{z}[0.05 + 1.05(1-z)^2], \quad (40)$$

and the gluon fragmentation function to pions,

$$D_G(z) = -0.1 - 2.1z + \frac{2.2}{z} + 4.2 \ln z\,. \quad (41)$$

As suggested earlier the gluon fragmentation function is "softer" than that of the quarks, $D_G(z) < D_j(z)$ for $z > 0.21$. This functional form for the gluons is obtained by assuming that the gluon first breaks up into a quark-antiquark pair, and then the quarks fragment into the observed hadrons. At large z_H, the hadrons from quark fragmentation will dominate. For the sake of simplicity we also neglect the QCD-induced scale dependence (renormalization) of these fragmentation functions. For the kinematic regime of interest we do not expect there to be a large variation and, in any case, this variation will largely cancel out in the ratio defining $\langle \cos\phi \rangle$.

To proceed we must deal with the fact that the perturbative expressions in Eqs. (36) and (38) are divergent as x and z approach 1. This limit corresponds to the situation when the emitted gluon is soft and is relevant whenever we include hadrons with small P_T in our calculation, i.e., for small values of the cutoff p_c. Such an infrared divergence is an artifact of the way we have treated the perturbative expansion. For a sufficiently inclusive quantity it would be canceled by the virtual-gluon contributions. In any case, the region where the difficulty arises

is where the fixed-order perturbative calculation is not valid. This is the regime that we expect to be described by the lowest-order perturbative result including intrinsic transverse momentum. In order to define a perturbative result that can interpolate over all regions of phase space, we control the integration of the order-α_s cross section so as to ensure that the contribution from the potentially singular region is bounded by the lowest-order contribution to the total (fully integrated) cross section. In particular, we require that the integration of the order-α_s contribution satisfy $\ln(1-x)\ln(1-z) < 3\pi/4\alpha_s$. The P_T cut p_c introduces a similar (but physically motivated) constraint of the form $(1-x)(1-z) > (p_c/z_H Q)^2$ [recall Eq. (11)]. Thus the former, *ad hoc* constraint is numerically relevant only for $p_c/Q \lesssim 0.01$. Except for astronomical values of Q this corresponds to the nonperturbative regime where the order α_s, perturbative contribution itself is not dominant. For larger values of p_c we obtain the usual perturbative result. Thus our *ad hoc* constraint is only technical and has no impact on the physics conclusions.

Perhaps the most interesting feature of our analysis is the amount of structure we see in the quantity $\langle\cos\phi\rangle$ as a function of the transverse momentum cutoff p_c. As suggested earlier nonperturbative effects are negligible at large values of p_c because the assumed intrinsic transverse momenta in the distribution and fragmentation functions are too small to produce $P_T > p_c$. Therefore $\langle\cos\phi\rangle$ exhibits structure as one goes from the region dominated by nonperturbative physics to the perturbative regime. This is illustrated in Fig. 5 where $\langle\cos\phi\rangle$ is plotted as a function of p_c along with recent data from the E665 Collaboration at Fermilab [4]. These data correspond to $Q^2 \geq 3.0$ GeV^2 with $\langle Q^2\rangle = 11.2$ GeV^2 and the ranges $0.003 \leq x_H \leq 0.15$, $0.2 \leq z_H \leq 1.0$ and $0.1 \leq y \leq 0.85$. The theoretical curves correspond to integrating over the same ranges. In order to make an average over the wide range of Q^2, we use the relation $Q^2 = 2MEx_Hy$, where M is the proton mass and E is the initial lepton energy in the lab frame. E is fixed at 490 GeV in the numerical analysis, while it is sharply peaked at 490 GeV in experiments. The various curves correspond to different values of the parameters a and b, defined in Eq. (21) and Eq. (24), respectively. We see that our simple Gaussian model for the intrinsic transverse momentum distributions describes the experimental data reasonably for $a \approx b \approx 0.6$ GeV. This corresponds to an average intrinsic transverse momenta of 0.53 GeV. For these parameter values, the nonperturbative result is less than 10% of the perturbative result when $p_c \geq 2.0$ GeV, and negligible for $p_c \geq 3.0$ GeV. However, nonperturbative effects cannot be neglected in the experimental data from E665 Collaboration, where they analyze samples of hadrons with the momentum cutoff smaller than 2.0 GeV.

An interesting feature of both the data and the theoretical model is the presence of a minimum (i.e., a maximum of the magnitude $|\langle\cos\phi\rangle|$) or dip at $p_c \approx 1.0$ GeV. For small values of p_c the nonperturbative contributions dominate and $|\langle\cos\phi\rangle|$ is an increasing function of p_c. For $p_c \gg 1.0$ GeV the nonperturbative effects are relatively

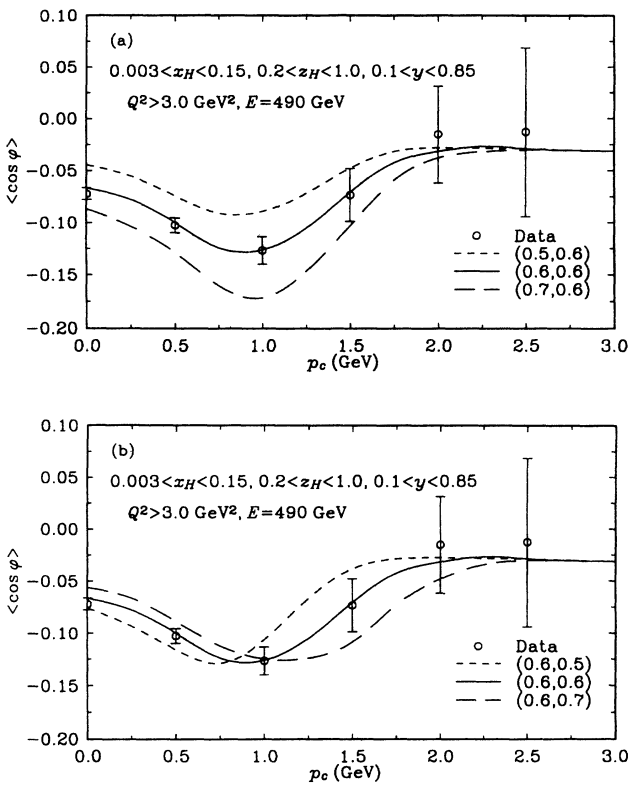

FIG. 5. $\langle\cos\phi\rangle$ for (a) various values of a with b=0.6 GeV and (b) various values of b with $a = 0.6$ GeV.

suppressed and the perturbative effects are dominant but exhibit a relatively small value for $|\langle\cos\phi\rangle|$. Hence the position of the dip in these low Q^2 data identifies the region where nonperturbative and perturbative effects are comparable.

In more detail, Fig. 5(a) displays results for fixed $b = 0.6$ GeV and varying a. For large a, the initial parton can have large transverse momentum. Since the nonperturbative effect is proportional to the magnitude of the transverse momentum, the magnitude of the nonperturbative $\langle\cos\phi\rangle$ should increase as a increases. This is clearly illustrated in Fig. 5(a). Figure 5(b) indicates that the behavior of $\langle\cos\phi\rangle$ as b varies, with fixed $a = 0.6$ GeV, is more complicated. As b increases, the position of the dip shifts to larger p_c with little variation in the magnitude of the effect. Although our model for the intrinsic transverse momentum distribution is an *ad hoc* construction, it seems to describe the experimental data reasonably with only two parameters. The values of these parameters that fit the data are also plausible, corresponding to intrinsic transverse momenta of the order of 500–600 MeV.

If we shift our focus to larger Q^2 values and larger transverse momenta for the hadrons, the nonperturbative contribution is much less important. The model results are no longer sensitive to the detailed assumptions about the intrinsic transverse momentum distribution. Figures 6(a) and 6(b) show $\langle\cos\phi\rangle$ for $Q = 10$ GeV, and 100 GeV, respectively, averaged over the ranges $0.05 \leq x_H \leq 0.15$, $0.2 \leq y \leq 0.8$ and $0.3 \leq z_H \leq 1.0$.

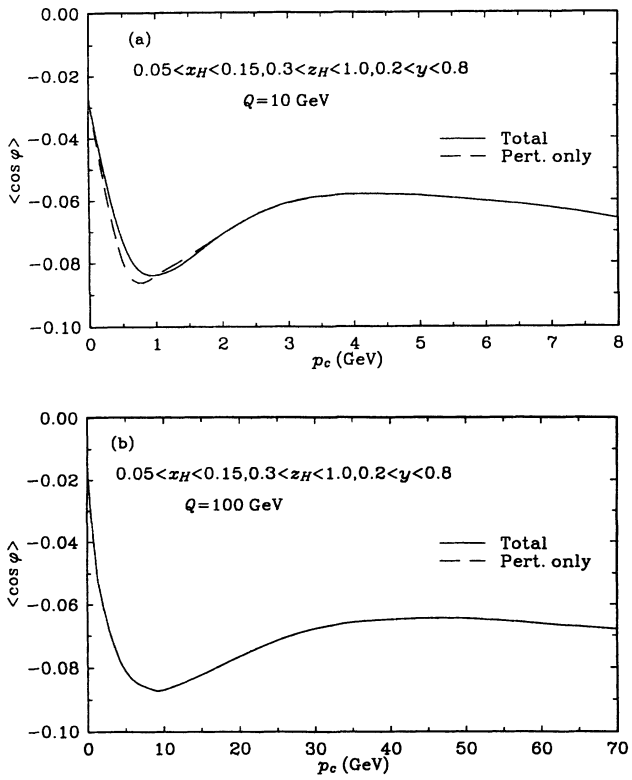

FIG. 6. $\langle\cos\phi\rangle$ for (a) $Q = 10$ GeV and for (b) $Q = 100$ GeV.

The solid line is the full expression for $\langle\cos\phi\rangle$ in Eq. (19) and the dashed line is the perturbative result of Eq. (34) [the two curves are effectively identical in Fig. 6(b)]. For either Q value and for $p_c \geq 2$ GeV, we see that nonperturbative effects are negligible. In this regime the perturbative results are also insensitive to our regularization procedure for the x and z integrals. On the other hand, $\langle\cos\phi\rangle$ still exhibits structure as a function of p_c. Its magnitude, $|\langle\cos\phi\rangle|$, still has a maximum but now at $p_c/Q \simeq 0.1$, approximately independent of Q. This perturbative structure was hidden by the dominant nonperturbative contribution in Fig. 5. We can understand this behavior qualitatively by considering the dependence on p_c of the numerator and denominator in Eq. (19) separately. Both are monotonically decreasing functions of p_c. However, for small p_c values the denominator (the total semi-inclusive cross section) initially falls much more rapidly than the numerator leading to an increasing $|\langle\cos\phi\rangle|$. For $p_c/Q > 0.1$ the denominator falls somewhat more slowly than the numerator until $p_c/Q > 0.5$ when the roles are again reversed. This structure leads to the observed feature that after the first maximum in $|\langle\cos\phi\rangle|$ there is a local minimum followed by a gradual increase. The detailed structure of this latter behavior is dependent on the relative role of all three processes [Eqs. (7), (8), and (9)] and may prove useful in isolating features of the gluon structure and fragmentation functions. By varying the choice of renormalization scale and the choice of structure functions, we estimate that the theoretical uncertainty in our results, due to higher orders in the perturbative expansion and uncertainties in the distribution and fragmentation functions, to be of order 10%. This high level of precision arises from the cancellation of effects in the ratio defining $\langle\cos\phi\rangle$. Detailed measurements of this quantity at HERA will provide both general and detailed tests of the underlying QCD structure.

VI. CONCLUSION

We have seen that a simple model calculation, including both the first nontrivial order in perturbative QCD and nonperturbative physics in the form of intrinsic transverse momentum in the lowest-order cross section, offers a simple understanding of existing data on the azimuthal structure of the hadronic final state in deep-inelastic ℓp scattering. In particular, we have analyzed the dependence of the azimuthal asymmetry parameter $\langle\cos\phi\rangle$ on the transverse momentum cutoff p_c, which defines the sample of hadrons. An attractive feature of this analysis in our simple model is that we are able to track the dependence on p_c over a kinematic range that encompasses both the nonperturbative and perturbative regimes. The study seems to nicely interpolate between earlier analyses that focused either on low values of p_c [9] or on larger values [10]. We note that the dependence of $\langle\cos\phi\rangle$ on p_c displays a remarkable amount of structure and matching this structure to the data serves to identify the transition region between nonperturbative and perturbative physics.

The model employs Gaussian distributions of intrinsic transverse momenta in both the initial and final states. For $p_c < 2$ GeV, $\langle\cos\phi\rangle$ depends sensitively on the width parameters of these Gaussians, a and b and thus on nonperturbative physics. The range of a and b values required to describe the present data imply average intrinsic transverse momenta in the reasonable region of 500–600 MeV. At large values of Q with $p_c > 2$ GeV, the details of the nonperturbative contributions do not matter since these contributions are suppressed. In this regime, $\langle\cos\phi\rangle$ is independent of α_s (at the order calculated here). However, $\langle\cos\phi\rangle$ displays nontrivial dependence on the momentum cutoff p_c that is characteristic of the nature of QCD and of the structure of the target hadrons.[2] In particular, the precise form of the dependence is a function of the spin of the exchanged gluon and of the relative contributions of the quarks and gluons in the target. Detailed measurements of $\langle\cos\phi\rangle$ versus p_c will provide detailed tests of our understanding of the strong interactions. Finally we have seen that the existing data for $\langle\cos\phi\rangle$ are predominantly in the nonperturbative regime but that perturbative QCD should dominate in the expected kinematic regime at HERA.

[2]We note that Monte Carlo simulations of the hadronic final states that neglect the correlations between the leptonic and hadronic parts of the scattering amplitude, which lead to the perturbative asymmetry, will be unable to produce the correct azimuthal angular dependence of the final-state hadrons.

ACKNOWLEDGMENTS

This work was supported in part by the U.S. Department of Energy, Contract No. DE-AS06-88ER40423. One of us (W.J.S.) is grateful to the University of Washington for financial support. We wish to thank Henry Lubatti and Douglas Jansen for discussing the data from the E665 Collaboration at Fermilab.

[1] H. Georgi and H.D. Politzer, Phys. Rev. Lett. **40**, 3 (1978).
[2] R.N. Cahn, Phys. Lett. **78B**, 269 (1978); Phys. Rev. D **40**, 3107 (1989).
[3] E.L. Berger, Phys. Lett. **89B**, 241 (1980).
[4] D. Jansen, Ph.D. thesis, University of Washington, 1991.
[5] R.K. Ellis *et al.*, Nucl. Phys. **B152**, 285 (1979).
[6] P.N. Harriman *et al.*, Phys. Rev. D **42**, 798 (1990).
[7] See, for example, A. König and P. Kroll, Z. Phys. C **16**, 89 (1982).
[8] L.M. Sehgal, in *Lepton and Photon Interactions at High Energies*, Proceedings of the International Symposium, Hamburg, West Germany, 1977, edited by F. Gutbrod (DESY, Hamburg, 1977), p. 837.
[9] See, for example, M. Arneodo *et al.*, Z. Phys. C **34**, 277 (1987).
[10] See, for example, P. Mazzanti, R. Odorico, and V. Roberto, Phys. Lett. **80B**, 111 (1978).